Formulation of a Low-Order Model of a Moist General Circulation

EDWARD N. LORENZ

Center for Meteorology and Physical Oceanography, Massachusetts Institute of Technology, Cambridge, MA 02139

(Manuscript received 26 July 1983, in final form 14 February 1984)

ABSTRACT

A two-layer quasi-geostrophic beta-plane model is converted into a moist general circulation model by including total water content as an additional prognostic variable. The water-vapor and liquid-water mixing ratios are determined diagnostically from the total-water mixing ratio and the saturation mixing ratio. The underlying surface is ocean, which exchanges water with the atmosphere through evaporation and precipitation. The circulation is driven by solar heating. Thermodynamic and radiative effects of water are included. The model is reduced to a low-order model by expressing each horizontal field in terms of seven orthogonal functions.

When horizontal variations of solar heating are suppressed, there are sometimes two stable steady states—a cold, rather cloudy state and a warm, nearly clear state. A cloud–albedo feedback process appears to be responsible for the multiple equilibria. With variable solar heating the model produces cyclones and anticyclones, with maxima of relative humidity and precipitation ahead of the cyclones, and minima ahead of the anticyclones.

1. Introduction

Many of the most important and influential recent works which dynamic meteorologists have acknowledged as belonging in their field, and which meteorological journals have accepted for publication, have dealt with the behavior of a gas of uniform composition. This situation might surprise a nonmeteorologist, since the most easily seen features of the real atmosphere, as is especially evident in these days of satellite photography, are the clouds, whose variable distribution in space and time demands a fluid of varying composition. The clouds are not mere atmospheric ornaments or tracers. The fact that they are visible implies that they reflect some of the sun's radiation which otherwise would penetrate to lower levels in the atmosphere and heat the ocean and land surfaces underneath, while, together with the water vapor which must be present if they are not to evaporate immediately, the clouds are strong absorbers and emitters of longwave radiation. Furthermore, the gain and release of latent heat, which must accompany changes in pressure and temperature if the clouds and water vapor are to remain in equilibrium, give moist air a different thermodynamic behavior from dry air. It is therefore relevant to ask to what extent the dry atmosphere which appears in so many theoretical studies is an acceptable model of an atmosphere where water in its gaseous, liquid and solid phases occurs in varying concentrations.

One can seek an answer by comparing the results of dry-atmosphere studies with observations of the real atmosphere, although it may remain uncertain whether the inevitable discrepancies are due to approximations other than the omission of water. Alternatively, one can compare dry-atmosphere studies with other theoretical studies where the presence of water enters explicitly. Such studies logically include the recent work with large global circulation models. However, to make their problems more manageable, dynamicists often construct less complicated models, where some real properties believed to be of secondary importance are purposely omitted. Additional labor is often saved by making the spatial resolution rather coarse. Models with the lowest resolution have become known as "low-order" models—a term introduced by Platzman (1960).

Many of the most familiar models are "low-order" in the vertical direction; one- and two-layer models continue to be popular. Models may be low-order in two directions; an example is a moist model of Held and Suarez (1978), which, however, retains considerable cross-latitude structure. A model may be called "very-low-order" if appreciable further reduction of the resolution in any direction would automatically eliminate some property or process which the investigator wishes to study, just as reduction from two layers to one eliminates baroclinic activity.

Very-low-order models cannot have as their purpose the quantitative duplication of real atmospheric behavior. Qualitatively they must reproduce some aspects of the behavior, if they are to serve any purpose. Often they are of pedagogical value; they can illustrate in an understandable manner the chain of events responsible for some phenomenon. Their chief use, however, may be exploratory; they can uncover new features or phenomena, which can subsequently be checked with more detailed models, or perhaps with real observations.

They can also provide great savings in computational effort.

The purpose of the present study is to construct a very-low-order model, capable of examining the difference between the global-scale behavior of a moist atmosphere and that of an atmosphere of uniform composition. Water-vapor and liquid-water content will appear in the moist model as dependent variables, and the physics of the model will include both the radiative and the thermodynamic effects of water. To obtain a dry model for comparison, we could take the moist model and equate the water content to zero, but we suspect that this would alter the field of radiative heating and cooling so drastically that the resulting circulation would be unrecognizably different. An alternative procedure is to remove only the thermodynamic effects of water, and evaluate the radiative effects which would occur with some prechosen uniform water distribution.

The construction of a low-order moist model entails certain difficulties. The radiative and thermodynamic processes which characterize a moist atmosphere both introduce complicated nonlinear terms into the governing dynamic equations. Low-order models are most frequently formulated by expressing the relevant fields as truncated series of spatially orthogonal functions, since, when sparsely distributed grid points are used instead, horizontal finite differences do not afford good approximations to horizontal derivatives. Simple products of series of orthogonal functions are easy to evaluate, but more complicated nonlinear functions are not.

In larger models using orthogonal functions this difficulty is often circumvented by transforming the variables from orthogonal-function space to grid-point space at each time step, evaluating the cumbersome nonlinear terms at each grid point, and then transforming back to orthogonal-function space, where the horizontal derivatives are evaluated. This procedure is also possible in a low-order model, but it introduces new difficulties. Because a global field of water vapor content possesses horizontal variations comparable to its mean value, the representation of a realistic field in terms of a small number of orthogonal functions, with coefficients which are optimal for the bulk of the atmosphere, is likely to yield supersaturation at some outlying grid points and negative moisture content at others. Neither outcome is tolerable.

We can avoid these difficulties by making a few departures from the most commonly used procedures. First, we shall use a quantity representing total water content rather than water vapor content as a basic dependent variable. We shall use a diagnostic equation to specify how much of the total water is vapor and how much is liquid; if this equation is judiciously chosen the problem of supersaturation will not arise.

Next, our variable representing total water content will be "total dew point" rather than total-water mixing ratio. By the total dew point we mean the value which the dew point would acquire if all the liquid water were converted to vapor. Like the temperature, the total dew point should vary by a factor of less than 2 in the horizontal direction, and even a highly truncated series of orthogonal functions should not yield negative values.

We anticipate performing experiments in which we shall alter the value of a constant, or the initial value of a dependent variable, by a very small amount, after which we shall determine the consequent change in some other quantities. To avoid possible bizarre results we shall insist that our equations be free of all discontinuities. In particular we shall formulate our diagnostic equation for water vapor so that, as air is lifted, there will be no abrupt change from dry adiabatic to moist adiabatic cooling. We can justify such a formulation by noting that each grid point actually represents a large area, and that a portion of this area may contain clouds while another portion is subsaturated.

With the many simplifications which we shall introduce, our model might more properly be regarded as a very-low-order model of some unspecified planet whose atmosphere contains some unspecified constituent which is present in varying concentrations and in more than one phase. Nevertheless, in making numerical computations we must choose numerical values for the physical constants, and we shall choose these to be representative of the earth's atmosphere, with water as the variable constituent.

In a recent article reviewing the general subject of very-low-order models (Lorenz, 1982), we described some features of an earlier version of the moist model, in order to demonstrate how certain difficulties encountered in the construction of models might be overcome. In the present article we shall describe the current version of the model in its entirety. After examining some preliminary numerical solutions we shall speculate on how future versions of the model might best be formulated.

2. The continuous equations

Our model atmosphere will be composed of a mixture of dry air, water vapor and liquid water in variable proportions. It will be of infinite upward and west–east extent, and will be bounded on the south and north by frictionless vertical walls. Under the atmosphere will be an ocean of uniform composition and limited vertical extent. The atmosphere will be governed by baroclinic, geostrophic, midlatitude beta-plane dynamics, while the ocean will exchange heat and water with the atmosphere. The sole external driving force will be incoming solar radiation; dissipation will be both thermal and mechanical. We shall not consider the possible presence of ice, even at subfreezing temperatures, nor shall we allow ocean currents to develop.

We shall first formulate the equations for a vertically and horizontally continuous atmosphere–ocean system. We shall next reduce the equations to those of a two-layer atmosphere and a single-layer ocean, by vertical averaging. Finally, we shall introduce a truncated set of orthogonal functions, in terms of which each horizontally continuous field will be expressed.

Our basic equations will contain the constants:

D distance between walls, divided by π,
p_0 mean sea-level pressure,
p_1 mean pressure at bottom of oceanic layer,
f Coriolis parameter midway between walls,
β northward derivative of Coriolis parameter,
c_p specific heat of air at constant pressure,
R gas constant for air,
L latent heat of condensation,
c specific heat of water,
R_W gas constant for water;

the independent variables:

t time,
x eastward distance,
y northward distance,
p pressure;

and the basic dependent variables:

$\tilde{\psi}$ streamfunction,
$\tilde{\chi}$ velocity potential,
$\tilde{\omega}$ individual pressure change,
$\tilde{T}$ atmospheric temperature,
$\tilde{W}$ total dew point, and
$\tilde{S}$ oceanic temperature.

The horizontal wind field will be the sum of a rotational nondivergent part, derivable from $\tilde{\psi}$, and an irrotational divergent part, derivable from $\tilde{\chi}$. To this list we shall add the auxiliary variables:

$\tilde{\tau}$ saturation mixing ratio at temperature $\tilde{T}$ and pressure p,
$\tilde{v}$ water vapor mixing ratio,
$\tilde{w}$ total-water mixing ratio, equal to saturation mixing ratio at temperature $\tilde{W}$ and pressure p, and
$\tilde{s}$ saturation mixing ratio at temperature $\tilde{S}$ and pressure p_0.

We have placed a tilde over each dependent variable because we shall be using the same symbols without tildes for the values of these variables at the atmosphere–ocean interface.

Our diagnostic equation for water vapor, which will distinguish our model from most other models, will be

$$(\tilde{\tau} - \tilde{v})(\tilde{w} - \tilde{v}) = \gamma^2 \tilde{v}^2, \tag{1}$$

where γ is a constant. This equation makes the liquid water content $\tilde{w} - \tilde{v}$ small when the degree of subsaturation $\tilde{\tau} - \tilde{v}$ is large, and vice versa, while the ratio of liquid water to vapor approaches zero as $w \to 0$. Choosing $\gamma = \frac{1}{4}$ makes the relative humidity $\tilde{r} = \tilde{v}/\tilde{\tau}$ equal to only 80% when $\tilde{\tau}$ and $\tilde{w}$ are equal, so that the water, if all vapor, would saturate the air; the remaining 20% of the water is in the form of clouds. When $\tilde{w}/\tilde{\tau} = 0.5$, $\tilde{v}/\tilde{\tau} = 0.473$. Should we wish to return to the conventional assumption that there is no supersaturation, and no cloudiness with subsaturation, we need merely set $\gamma = 0$; this will, however, introduce the discontinuity which we prefer to avoid. Alternative equations with similar properties could presumably be formulated.

The mixing ratios $\tilde{\tau}$, $\tilde{w}$ and $\tilde{s}$ will be related to the basic variables by the diagnostic equations

$$\tilde{\tau} = c'\tilde{T}^{\mu}/p, \tag{2}$$

$$\tilde{w} = c'\tilde{W}^{\mu}/p, \tag{3}$$

$$\tilde{s} = c'\tilde{S}^{\mu}/p_0, \tag{4}$$

where μ is a constant and c' is to be chosen to produce the desired saturation mixing ratio at some standard temperature and pressure. Equations (2)–(4) may be derived from the familiar Clausius–Clapeyron equation if the factor $\tilde{T}^2$ in that equation is first replaced by the product $T_s\tilde{T}$, where T_s is a standard temperature typical of the atmosphere, say 273 K. An appropriate value for the exponent $\mu = L/(R_W T_s)$ is then about 20.0. Making $\tilde{\tau}$ proportional to a high power of $\tilde{T}$ assures us that the moist adiabatic lapse rate will be close to the dry adiabatic when $\tilde{T}$ is low, but considerably smaller when $\tilde{T}$ is high. Making μ an integer effects a significant reduction in computation time.

The basic prognostic equations will be the vorticity equation

$$\partial\nabla^2\tilde{\psi}/\partial t + J(\tilde{\psi}, \nabla^2\tilde{\psi}) + \beta\partial\tilde{\psi}/\partial x = -f\nabla^2\tilde{\chi} + F, \tag{5}$$

the atmospheric thermodynamic equation

$$d(c_p\tilde{T} + L\tilde{v})/dt = R\tilde{T}\tilde{\omega}/p + H, \tag{6}$$

the water-content equation

$$d\tilde{w}/dt = G, \tag{7}$$

and the oceanic thermodynamic equation

$$d(c\tilde{S})/dt = E. \tag{8}$$

Here J denotes a Jacobian with respect to x and y, while the diabatic terms F, H, G and E denote, respectively, the curl of the viscous drag, the atmospheric diabatic heating per unit mass (including the effect of evaporation from the ocean surface, but not condensation within the atmosphere, which increases $\tilde{T}$ but decreases $\tilde{v}$), the gain or loss of water by evaporation or precipitation, and the oceanic heating per unit mass. Note that (7) has been formulated in terms of $\tilde{w}$ rather than $\tilde{W}$. In keeping with the geostrophic simplification we have omitted the advection of vorticity by the divergent part of the wind, but we implicitly include the

complete advection of enthalpy and water in the time derivatives in (6) and (7); we do so because we feel that an important possible feature of a moist general circulation is the accumulation of water at low levels in low latitudes brought about by a Hadley circulation, which is divergent.

Equations (5)–(8) are to be accompanied by the diagnostic continuity and thermal-wind equations

$$\partial\tilde{\omega}/\partial p = -\nabla^2\tilde{\chi}, \tag{9}$$

$$\partial\tilde{\psi}/\partial p = -R\tilde{T}/(fp). \tag{10}$$

Equation (10) implies that the horizontal average of $\tilde{\psi}$ increases with elevation, and that, aside from a constant factor, $\tilde{\psi}$ is the isobaric height. For boundary conditions we shall let $\tilde{\omega} = 0$ when $p = 0$ or p_0. Equations (1)–(10) form a closed system in the ten dependent variables.

At this point it is convenient to convert to dimensionless quantities. To do this we choose $1/f$, D, p_0 and D^2f^2/R as the units in which time, distance, pressure and temperature are measured. We then redefine each symbol, including ∇ and J, as the ratio of the quantity originally defined by the symbol to the combination of f, D, p_0 and R with the appropriate dimensions. In the equations which follow we shall assume, unless we state otherwise, that all quantities have been made dimensionless. Since f, D, p_0 and R then all equal unity, we can omit them when they occur as factors.

3. Vertical simplification

In many two-level or two-layer atmospheric models the stream-function is specified at each of two levels, or averaged through each of two layers, while the temperature is specified for only one level or layer. The temperature is then identified through the thermal wind equation with the difference of the stream functions. We shall use the two-streamfunction one-temperature format in our model. It is consistent with this formulation to specify the total dew point for only one level or layer.

Our procedure for reducing Eqs. (1)–(10) to a layered model will be dictated by a consideration of the source and sink terms F, H, G and E. It is not at all obvious how these should be formulated at individual levels within the atmosphere or ocean. However, if horizontal diffusive exchanges of momentum, energy and water are considered negligible, the vertical averages of F, H, G and E simply represent net exchanges between the atmosphere and the ocean, and, in the case of energy, between the atmosphere or the ocean and outer space. Accordingly, we shall construct our vertically simplified model by averaging Eqs. (6)–(8) through the depth of the atmosphere or ocean. Equation (5) must be averaged through two separate layers in order to yield two streamfunctions, so that the exchange of momentum between these layers will also enter the model.

Because $\tilde{\tau}$, $\tilde{v}$ and $\tilde{w}$ normally fall off much more rapidly with elevation than $\tilde{T}$ and $\tilde{W}$, we cannot locate a particular level at which the values of the various terms in (5)–(7) are all suitable substitutes for vertical averages. We shall therefore specify the manner in which each dependent variable varies with p, whereupon vertical averaging will be feasible. We shall find it convenient to express the dependent variables in terms of their values at the atmosphere–ocean interface; these will be denoted by symbols without tildes, and will become our new dependent variables.

We first let the lapse rate of atmospheric temperature with elevation be constant, so that

$$\tilde{T} = Tp^{\lambda}, \tag{11}$$

where λ is a constant. We make no attempt to model a stratosphere. Since $\lambda = 0$ would imply an isothermal stratification, and $\lambda = \kappa = R/c_p$ would imply a dry-adiabatic lapse rate, λ should lie between 0 and κ. We omit all vertical variations of oceanic temperature, since we are considering a relatively shallow layer, so that

$$\tilde{S} = S. \tag{12}$$

It follows from (10), (2) and (4) that

$$\tilde{\psi} = \psi + T(1 - p^{\lambda})/\lambda, \tag{13}$$

$$\tilde{\tau} = \tau p^{\mu\lambda-1}, \tag{14}$$

$$\tilde{s} = s. \tag{15}$$

Next we let $\tilde{r} = \tilde{v}/\tilde{\tau}$ be constant within each vertical column, thus $\tilde{r} = r$. Then

$$\tilde{v} = vp^{\mu\lambda-1}. \tag{16}$$

Equation (1), being homogeneous in $\tilde{\tau}$, $\tilde{v}$ and $\tilde{w}$, still holds when the tildes are dropped, so that

$$\tilde{w} = wp^{\mu\lambda-1}, \tag{17}$$

whence, from (3),

$$\tilde{W} = Wp^{\lambda}. \tag{18}$$

In order that $\tilde{w}$ remain finite as the top of the atmosphere is approached, it is necessary that $\lambda \geqslant \nu$, where $\nu = 1/\mu$.

Finally, we let $\tilde{\chi}$, like $\tilde{\psi}$, be linear in p^{λ}, so that, if (5) is to be satisfied, with $\tilde{\omega} = 0$ when $p = 0$ or 1,

$$\tilde{\chi} = \chi\{-1 + (1 + \lambda)p^{\lambda}\}/\lambda, \tag{19}$$

$$\tilde{\omega} = \nabla^2\chi(p - p^{1+\lambda})/\lambda. \tag{20}$$

We may treat Eqs. (11)–(20) as approximations to be used only for vertical averaging, or we may assume that F, H, G and E implicitly include internal processes which serve to maintain the prescribed vertical distributions against the disruptive effects of advection and other processes, just as vertical motion and divergence serve to maintain hydrostatic and geostrophic equilibrium against the disruptive effects of various processes.

We shall average Eq. (5) separately from $p = 0$ to 1 and $p = 0$ to a level λ'; this is equivalent to averaging from 0 to λ' and λ' to 1. The most logical value of λ' would probably be $\frac{1}{2}$, but it makes the equations slightly simpler to let $\lambda' = (1 - \lambda)^{1/\lambda}$, or, for acceptable values of λ, about $\frac{1}{3}$. We then find that two linear combinations of the averaged equations are

$$\partial\nabla^2\psi/\partial t + J(\psi, \nabla^2\psi) - a_\psi J(T, \nabla^2 T) + \beta\partial\psi/\partial x = -\nabla^2\chi + 2\bar{\bar{F}} - \bar{F}, \quad (21)$$

$$\partial\nabla^2 T/\partial t + J(\psi, \nabla^2 T) + J(T, \nabla^2\psi) + a_T J(T, \nabla^2 T) + \beta\partial T/\partial x = (1 + \lambda)\nabla^2\chi - (1 + \lambda)(\bar{\bar{F}} - \bar{F}), \quad (22)$$

where $a_\psi = 1/(1 + 2\lambda)$, $a_T = (3 + \lambda)a_\psi$, and the double and single bars over F denote averages from 0 to 1 and 0 to λ', respectively.

Averaging Eq. (6), *after* using (1), (2) and (7) to express $d\tilde{v}/dt$ in terms of $d\tilde{T}/dt$ and G, we obtain

$$(1 + \alpha)\{\partial T/\partial t + J(\psi, T)\} = -(b_T + b_W\alpha)\nabla T\cdot\nabla\chi + (c_T - c_W\alpha)T\nabla^2\chi + (1 + \lambda)(\bar{\bar{H}} - \partial v/\partial w L\bar{\bar{G}})/c_p, \quad (23)$$

where

$$b_T = -\lambda a_\psi, \quad b_W = \frac{1 - \nu/\lambda}{1 + \nu},$$

$$c_T = (\kappa - \lambda)a_\psi, \quad c_W = \nu b_W,$$

$$\alpha = \left(1 + \frac{1}{\lambda}\right)\frac{\partial v}{\partial\tau}\left(\frac{L}{c_p}\right)\frac{\tau}{T}, \quad (24)$$

and the partial derivatives $\partial v/\partial\tau$ and $\partial v/\partial w$ are to be evaluated from (1). Averaging Eq. (7), and then using (3) to express w in terms of W, we obtain

$$\frac{\partial W}{\partial t} + J(\psi, W) + a_W J(T, W) = -b_W\nabla W\cdot\nabla\chi - c_W W\nabla^2\chi + \lambda(W/w)\bar{\bar{G}}, \quad (25)$$

where $a_W = \nu/\{\lambda(1 + \nu)\}$. Finally, Eq. (8) becomes

$$dS/dt = \bar{\bar{E}}/c. \quad (26)$$

With the auxiliary variables τ, v, w and s defined by (1)–(4), applied at $p = 1$, and with the definition (24), Eqs. (21)–(23) and (25)–(26) become a closed system in the basic dependent variables ψ, χ, T, W and S.

The thermodynamic effects of water are incorporated in α. The factor $\partial v/\partial\tau$ in α is a function of r, and increases from 0 to 1 with increasing r; with $\gamma = 0$ it would change abruptly from 0 to 1 at the saturation point. The dry model [Eqs. (21)–(23), with $\alpha = 0$] differs little from other two-layer models. Potential vorticity is still advected at two levels; with $\lambda = 0.175$ and $p_0 = 1000$ mb, these levels are 679 and 88 mb. Moisture is advected with the wind at 642 mb, but the layer which radiates to space is often far above the 500 mb level.

4. Horizontal simplification

Low-order models of dry global-scale circulations are typified by a two-layer model which we introduced some time ago (Lorenz, 1963) to study the phenomenon of vacillation. In that model we expressed each horizontal field as a series of orthogonal functions truncated to seven terms; specifically, in a somewhat different notation, we introduced the approximation

$$X = \sum_{n=0}^{6} X_n\Phi_n, \quad (27)$$

where X stands for any dependent variable, and

$$\left.\begin{aligned}\Phi_0 &= 1\\ \Phi_{3j-2} &= 2\sin jy\cos 2x\\ \Phi_{3j-1} &= 2\sin jy\sin 2x\\ \Phi_{3j} &= \sqrt{2}\cos jy\end{aligned}\right\}, \quad (28)$$

where $j = 1$ or 2. The orthogonal functions Φ_n were chosen so that

$$\nabla^2\Phi_n = -a_n\Phi_n, \quad (29)$$

where $a_0 = 0$, $a_1 = a_2 = 5$, $a_3 = 1$, $a_4 = a_5 = 8$ and $a_6 = 4$. They satisfy the orthonormality conditions

$$[\Phi_m\Phi_n] = \delta_{mn}, \quad (30)$$

where the square brackets denote a horizontal average, whence the coefficients in (27) satisfy

$$X_n = [X\Phi_n]. \quad (31)$$

We then converted each horizontally continuous partial differential equation into a set of seven ordinary differential equations, by first substituting (27), for each dependent variable X, into each continuous equation, then expressing the left and right sides of each resulting equation in terms of orthogonal functions, using (31), and finally equating coefficients of $\Phi_0, \ldots, \Phi_6$. In the present model we shall express the basic dependent variables ψ, χ, T, W and S in terms of the same set of orthogonal functions. We may, in fact, regard the present model as an extension of the earlier model to a moist atmosphere.

Strictly speaking we should not express χ in terms of $\Phi_0, \ldots, \Phi_6$, since the y-derivative of χ should vanish at the boundaries $y = 0$ and π, while it is the x-derivatives of $\Phi_0, \ldots, \Phi_6$ which vanish there. We shall presently consider how the model would be changed by expressing χ in terms of more appropriate functions.

In the earlier model the right-hand sides of the continuous equations contain terms of the form $J(X, Y)$, to be expressed in terms of orthogonal functions. Approximating these terms by

$$J(X, Y) = \sum_{n=0}^{6}\Big(\sum_{j,k=0}^{6} J_{njk}X_jY_k\Big)\Phi_n, \quad (32)$$

we find from (31) that

$$J_{njk} = [\Phi_n J(\Phi_j, \Phi_k)]. \quad (33)$$

It follows that J_{njk} is unchanged by any cyclic permutation of (n, j, k) and changed only in sign by any noncyclic permutation, and, with our choice of orthogonal functions, $J_{123} = -5b$, $J_{156} = J_{426} = -8b$, $J_{453} = -4b$, and $J_{njk} = 0$ if (n, j, k) is not a permutation of (1, 2, 3), (1, 5, 6), (4, 2, 6) or (4, 5, 3). Here $b = 16\sqrt{2}/(15\pi)$.

In the present model we have additional quadratic terms of the form XY and $\nabla X \cdot \nabla Y$. Approximating XY by

$$XY = \sum_{n=0}^{6} \left(\sum_{j,k=0}^{6} I_{njk} X_j Y_k \right) \Phi_n, \quad (34)$$

we find that

$$I_{njk} = [\Phi_n \Phi_j \Phi_k]. \quad (35)$$

It follows that I_{njk} is unchanged by any permutation of (n, j, k) and, with our choice of orthogonal functions, $I_{0jj} = 1$ for all j, $I_{314} = I_{325} = I_{336} = -I_{611} = -I_{622} = 1/\sqrt{2}$, and $I_{njk} = 0$ if (n, j, k) is not a permutation of $(0, j, j)$, (3, 1, 4), (3, 2, 5), (3, 3, 6), (6, 1, 1) or (6, 2, 2). Since

$$\nabla X \cdot \nabla Y = \frac{1}{2} \{\nabla^2(XY) - X(\nabla^2 Y) - (\nabla^2 X) Y\}, \quad (36)$$

the appropriate approximation for $\nabla X \cdot \nabla Y$ is

$$\nabla X \cdot \nabla Y = \sum_{n=0}^{6} \left(\sum_{j,k=0}^{6} K_{njk} X_j X_k \right) \Phi_n, \quad (37)$$

where

$$K_{njk} = \frac{1}{2} (a_j + a_k - a_n) I_{njk}. \quad (38)$$

As already noted, to evaluate the more complicated nonlinear functions appearing in the source and sink terms, and in the moist-thermodynamic terms, it is preferable to transform from orthogonal functions to grid points, using (27), evaluate the nonlinear terms at each grid point, and then transform back, using (31). We have chosen a set of nine grid points, at the intersections of the lines $x = \pi/6$, $3\pi/6$ and $5\pi/6$ with the lines $y = \pi/6$, $3\pi/6$ and $5\pi/6$. We have found no way to get by with fewer than nine points.

Our model contains no prognostic equation for χ. To integrate the equations, we must eliminate $\partial T/\partial t$ from (22) and (23), and solve the resulting diagnostic "ω-equation" for χ. Although some of the terms must first be evaluated in grid-point space, the equation, which contains horizontal derivatives of χ, is not suitable for solution in grid-point space, and special care must be taken to make it readily solvable even in orthogonal-function space.

We note first that if ∇^{-2} denotes the particular inverse of ∇^2 whose horizontal average vanishes, (22) may be written

$$\partial(T - T_0)/\partial t = (1 + \lambda)(\chi - \chi_0) + \nabla^{-2} F', \quad (39)$$

where F' denotes all the terms in (22) which contain neither χ nor a time derivative. The horizontal average χ_0 of χ does not enter the dynamics and therefore may be chosen at will, and we can gain conciseness by equating χ_0 to $(\partial T_0/\partial t)/(1 + \lambda)$. When we then eliminate $\partial T/\partial t$ from (39) and (23), after dividing (23) by $b_T + b_W \alpha$, the resulting ω-equation may be written

$$A\chi - B\nabla^2 \chi + \nabla T \cdot \nabla \chi = H', \quad (40)$$

where A and B are algebraic functions of α, and H' represents the combined contribution of F' and all terms in (23) containing neither χ nor a time derivative.

Upon transforming to orthogonal functions, we obtain the seven linear algebraic equations

$$\sum_{k=0}^{6} \sum_{j=0}^{6} I_{njk} \left\{ A_j + a_k B_j + \frac{1}{2} (a_j + a_k - a_n) T_j \right\} \chi_k = H'_n, \quad (41)$$

to be solved for $\chi_0, \ldots, \chi_6$. The value of χ_0 gives us $\partial T_0/\partial t$, while $\chi_1, \ldots, \chi_6$ may be substituted into the transformed forms of (21), (22) and (25) to yield the time derivatives of ψ_n $(n \neq 0)$, T_n $(n \neq 0)$ and W_n. Equation (26) for S does not contain χ and presents no additional problems, while ψ_0, which is proportional to the horizontally averaged 1000 mb height, is assumed to vanish.

As we noted earlier, χ, when expressed in terms of $\Phi_0, \ldots, \Phi_6$, fails to satisfy the proper boundary conditions. One acceptable procedure would be to express $\nabla^2 \chi$ in terms of $\Phi_0, \ldots, \Phi_6$. The corresponding expression for χ would then contain correction terms involving hyperbolic sines and cosines; specifically, we would have

$$\chi = \sum_{n=0}^{6} \chi_n \Phi'_n, \quad (42)$$

where

$$\left.\begin{aligned} \Phi'_1 &= \left\{ 2 \sin y + \frac{\cosh(2y - \pi)}{\sinh \pi} \right\} \cos 2x \\ \Phi'_4 &= \left\{ 2 \sin 2y - \frac{2 \sinh(2y - \pi)}{\cosh \pi} \right\} \cos 2x \end{aligned}\right\}, \quad (43)$$

with analogous expressions for Φ'_2 and Φ'_5, while $\Phi'_n = \Phi_n$ if $n = 0$, 3 or 6.

Since we would not be changing $\nabla^2 \chi$, changes in the model would be confined to $\nabla T \cdot \nabla \chi$ in (23) and $\nabla W \cdot \nabla \chi$ in (25), which represent advection of heat and water by the divergent part of the wind—processes which are omitted altogether in many models. These changes will show up as changed numerical values of K_{njk} in (37).

These values are integrals over the entire channel. Examination of the correction terms in (43) shows that they are rather small, except in rather narrow latitude

bands near $y = 0$ and π, and that their contribution to integrals from 0 to π is likely to be of secondary importance. We shall therefore adopt the simple procedure of neglecting the corrections to K_{njk} altogether.

5. Sources and sinks

As we have already remarked, the vertical averages of F, H, G and E represent vertical exchanges of momentum, sensible and latent heat, and water. We shall assume that the exchanges across the ocean–atmosphere interface are proportional to the differences of appropriate quantities across this interface, with the same factor of proportionality k. We could appeal to Ekman-layer theory to determine a suitable value for k, but, in view of the drastic simplifications already introduced, we can hardly justify anything more involved than simply choosing a time constant, say five days, for $1/k$. Exchanges of momentum across the surface $p = \lambda'$, where there is no Ekman layer, will be made proportional to the shear, with a damping coefficient k' considerably smaller than k.

To formulate precipitation we assume that clouds have a "half life," i.e., that during a specified time interval they give up a specified fraction of their water as rain. The damping time $1/l$ should be considerably shorter than $1/k$, perhaps one day. Denoting the radiative contributions to H and E by H_R and E_R, we have

$$\bar{F} = -k\nabla^2\psi, \tag{44}$$

$$\bar{F} = -k'\nabla^2 T, \tag{45}$$

$$\bar{H} = -k\{c_p(T - S) + L(v - s)\} + \bar{H}_R, \tag{46}$$

$$\bar{G} = -k(v - s) - (lv/\lambda)(w - v), \tag{47}$$

$$\bar{E} = -\left(\frac{p_0}{p_1 - p_0}\right)k\{c_p(S - T) + L(s - v)\} + \bar{E}_R. \tag{48}$$

The factor v/λ appears in the precipitation term in (47) because the vertical average of $\tilde{w}$ is $(v/\lambda)w$.

Radiation is traditionally a complicated process, and, despite our efforts at simplification, our formulation will reflect this fact. Even if we are interested only in some atmosphere with some absorbing constituent, the appropriate radiation formulas will be highly dependent upon what this constituent is, and our radiation formulas, to a greater extent than our other expressions, will be based upon the supposition that it is water.

We shall express the incoming solar radiation in terms of a planetary temperature T^*; this is the temperature which a blackbody covering the entire sky would have to have, in order to be locally equivalent to the sun. We shall allow some of the incoming solar radiation to be reflected by clouds; the remainder will pass through the atmosphere and heat the ocean. We shall let the fractional cloud cover a be a function of the relative humidity. This appears preferable to letting a depend upon total water content; we are not aware, for example, that the tropics are much cloudier than the polar regions. As a first approximation we shall let the cloud albedo equal the fractional cloud cover a. A function which appears to produce a reasonable global average albedo is $a = r^4$.

The ocean will in turn emit longwave radiation as a blackbody. The cloud-free portion of the atmosphere will be assumed to possess a spectral window, through which a fixed fraction a' of the longwave radiation will pass; the remaining longwave radiation will be partially absorbed and reemitted by atmospheric water vapor. The cloudy portion of the atmosphere will behave like the cloud-free portion, except that there will be no spectral window.

Our expressions for emission of longwave radiation will need to contain the atmosphere's fractional emissivity, and the temperature at which the emission occurs. In a model with such low vertical resolution we balk at considering the radiative transfer from level to level, and find no reason for using anything more complicated than Simpson's method. Basically, Simpson (1928) treated the atmosphere as completely transparent in the 8.5–11 μm band (the window), while below 7 and above 14 μm he treated any layer containing 0.3 kg of water per m^2 of cross section as completely opaque. Simpson's atmosphere would therefore radiate to space in the latter wavelengths at the temperature of the uppermost such layer. Between 7 and 8.5, and between 11 and 14 μm, more water vapor would be needed to render the atmosphere opaque.

Paraphrasing Simpson's treatment, we shall as a first approximation allow the cloud-free portion of the atmosphere to radiate upward and downward at temperatures T' and T'', respectively, with the fraction $1 - a'$ of the intensity of blackbody radiation, while it will absorb the fraction $1 - a'$ of the radiation it receives from the ocean. We shall neglect any variations of a' which ought to occur with temperature. We shall treat the cloud-covered portion of the atmosphere similarly, except that a' will be replaced by 0. The temperatures T' and T'' will occur at pressures p' and p'', which will be the pressure levels above and below which the amount of water vapor is $V_s/2$, where $V_s = 0.3$ kg m^{-2}. Thus p' and p'' are supposed to represent the centers of the uppermost and lowermost layers whose water vapor content is V_s. Letting v_s be the value which v would possess if the water vapor content of an entire column were V_s, i.e., $v_s = (\lambda/v)gV_s/p_0$, where g is the acceleration of gravity, we obtain for our first approximation, using (16),

$$p' = \left(\frac{1}{2}\,v_s/v\right)^{v/\lambda}, \tag{49}$$

$$p'' = \left(1 - \frac{1}{2}\,v_s/v\right)^{v/\lambda}. \tag{50}$$

Equations (49) and (50) are fairly satisfactory if v/v_s is large, but if $v < v_s/2$ they place the uppermost layer with a water content of V_s *below* the lowermost layer, while in actuality such layers do not exist at all. We shall therefore modify (49) and (50) by replacing v with $v + v_s$. Introducing the ratio $v' = v/(v + v_s)$, which is near unity when v is large but is small when v is small, we find that

$$p' = \left(\frac{1}{2} - \frac{1}{2}v'\right)^{\nu/\lambda}, \tag{51}$$

$$p'' = \left(\frac{1}{2} + \frac{1}{2}v'\right)^{\nu/\lambda}, \tag{52}$$

whence

$$T' = T\left(\frac{1}{2} - \frac{1}{2}v'\right)^{\nu}, \tag{53}$$

$$T'' = T\left(\frac{1}{2} + \frac{1}{2}v'\right)^{\nu}. \tag{54}$$

Equations (51) and (52) are almost identical to (49) and (50) when v is large, but they make p' and p'' approach one another as $v \to 0$.

The assumption that the intensity of the radiation is $1 - a'$ times that of blackbody radiation also becomes unrealistic when v is small, since there is very little water vapor to radiate. Likewise, a sufficiently tenuous cloud layer should not radiate as a blackbody. We shall adjust for this situation by multiplying the emitted and absorbed radiation by v'. Finally, a tenuous cloud layer should not be a complete reflector of solar radiation, and we shall multiply a by v' to obtain the cloud albedo.

Collecting our results, and letting $a'' = a + (1 - a) \times a'$, we find that

$$\tilde{H}_R = (\sigma g/p_0)v'a''(S^4 - T''^4 - T'^4), \tag{55}$$

$$\tilde{E}_R = \{\sigma g/(p_1 - p_0)\}\{-S^4 + v'a''T''^4 + (1 - v'a)T^{*4}\}, \tag{56}$$

where σ is the Stefan–Boltzman constant.

6. Preliminary computations

A necessary final step in the development of our model is the performance of enough computations to assure us that the model is not completely unable to serve its purpose. Once we have discovered the model's capabilities and limitations we can engage in production runs.

With a typical low-order dry model the problem of finding an equilibrium solution, when the external heating is horizontally uniform, is trivial, but, with our moist model, the appropriate values of T, W and S are not at all obvious. Discovering how these quantities vary with T^* would appear to be a prerequisite to understanding the model.

Our problem consists of solving the algebraic equations obtained by equating F, H, G and E to zero, and the lazy way to solve them is to solve the model equations numerically with arbitrarily chosen initial conditions. We anticipate that ψ will vanish, while T, W and S will be horizontally uniform, so that instead of transforming back and forth between grid points and orthogonal functions we can work with a single grid point.

A necessary prelude to numerical computation is the selection of numerical values for the various constants. We shall choose our values with the earth's atmosphere and ocean in mind, but, to reduce the time needed for transient effects associated with the chosen initial conditions to disappear, we shall make the oceanic layer interacting with the atmosphere very thin. We might even regard the underlying surface as wet land rather than ocean.

The dimensionless values of f, D, p_0 and R are all unity. Our chosen dimensional values will be $1/f = 3$ h, $D = 1830$ km, $p_0 = 1000$ mb, and $R = 287$ $m^2\ s^{-2}\ K^{-1}$. These values have the practical advantage of making the unit for temperature exactly 100 K.

Dimensionless values of the remaining constants, or, where sufficient, combinations of constants, follow. We shall use these values in our numerical runs except where we indicate otherwise:

λ	0.175
μ	20.0
ν	0.05
κ	$2/7$
c_p	3.5
L	25.0
β	0.3
c'	$0.0038/(2.73^{20})$
γ	0.25
k	0.015
k'	0.003
lv/λ	0.03
c''	1.0
a'	0.5
v_s/λ	0.0006
$\sigma g/(c_p p_0)$	0.000061.

For various values of T^* we have performed runs where initially $\psi = 0$ and $T = W = S = T^*$, allowing each run to proceed until equilibrium is reached or easily extrapolated. Table 1 shows the results. An obvious feature is the large range of T, W and S, which are very high when T^* is high and very low when T^* is low. In addition, r and a are high and S and W exceed T when T is low, and the opposite is true when T is high, while S always exceeds W.

Once observed, these features are readily explained in the context of the model, regardless of whether they would occur in nature. First, since we have chosen lv/λ to exceed k, Eq. (47) with $G = 0$, representing a balance between evaporation and precipitation, expresses w as a weighted average of v and s, and, since $v < w$ always, $s > w$, whence $S > W$.

TABLE 1. Equilibrium values approached by T, W and S (K), and by r and a (%), in the low-order model when T^* is horizontally uniform and $T = W = S = T^*$ initially.

T^*	T	W	S	r	a
264.0	245.2	246.6	249.3	84.1	50.0
267.0	247.9	249.3	252.1	84.1	50.0
270.0	251.1	252.5	255.3	84.1	50.0
273.0	255.5	256.8	259.7	83.7	49.1
276.0	301.6	296.7	298.2	64.7	17.5
279.0	312.8	305.4	306.5	57.2	10.7
282.0	320.9	311.5	312.4	51.7	7.2
285.0	328.0	316.7	317.5	47.0	4.9

Next, starting from a cold equilibrium state, suppose that T, W and S increase by the same factor, so that r and a remain fixed. The latent heat transferred to the atmosphere, which is proportional to $s - v$, would then increase as T^{20}, while the heat lost by radiation or sensible heat transfer would increase only as T^4 or T, and equilibrium would no longer exist. To maintain a balance T would have to increase more rapidly than S, and hence ultimately more rapidly than W, since W is bounded by S. Hence r and a would decrease. Warm equilibria thus tend to be dry equilibria.

The abrupt increase in T, W and S as T^* increases from 273 to 276 K is completely out of line with the other increments. Indeed, if we plot T against T^* and attempt to draw a smooth curve through the points, it is difficult not to make it S-shaped. This suggests that, corresponding to some values of T^*, there may be two stable equilibria, with an unstable equilibrium in between.

We have attempted to locate the remaining equilibria by performing additional runs with new initial conditions. The result is the heavy curve in Fig. 1. The large dots indicate where runs were performed. Multiple equilibria occur when T^* is between 274.5 and 276 K. The unstable equilibrium represented by the dot at $T^* = 275.3$, $T = 277.5$ was located by a trial and error procedure.

The multiple equilibria appear to result from a positive cloud–albedo feedback process. If we had formulated the model with a constant albedo, T would increase in response to an increase in T^*. We have seen that as the model is presently formulated, the albedo a would decrease, allowing the solar heating to increase T still more, whence a would decrease still more, and so on. Under suitable conditions this might be a runaway process, i.e., an equilibrium might be unstable. Ultimately a new equilibrium would be reached, since a cannot decrease below zero.

We have tested this idea by performing additional runs in which the cloud albedo is held fixed, first at $0.1296 = 0.6^4$ and subsequently at $0.4096 = 0.8^4$. The absorption and emission of longwave radiation are still computed for a cloud cover of r^4. The result is the pair of thin curves in Fig. 1. There is no sign of multiple equilibria, and the upper curve is in fact nearly straight.

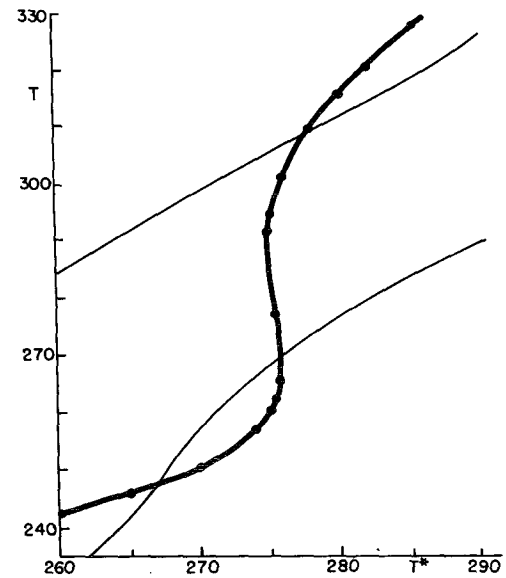

FIG. 1. Equilibrium temperature T corresponding to assigned horizontally uniform planetary temperature T^*, as given by the model. Heavy curve: albedo dependent on relative humidity. Upper thin curve: fixed low albedo. Lower thin curve: fixed high albedo.

If we let lv/λ equal 0.015 instead of 0.03, Eq. (47) with $G = 0$ assumes the even simpler form $s = w$, whence $S = W$. Since such a simple relation might facilitate the subsequent interpretation, we have repeated the runs which produced the heavy curve in Fig. 1, with the new value of l. The result is the right-hand heavy curve in Fig. 2. Multiple equilibria now

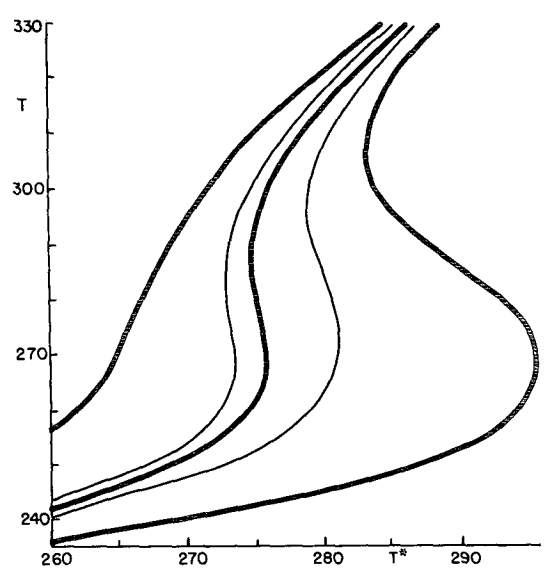

FIG. 2. Equilibrium temperature T corresponding to assigned horizontally uniform planetary temperature T^*, as given by the model, with albedo dependent on relative humidity. Left heavy curve: medium k, high l. Left thin curve: low k, medium l. Central curve: medium k, medium l. Right thin curve: high k, medium l. Right heavy curve: medium k, low l.

cover a wide range of values of T^*, and the two stable-equilibrium values of T are invariably separated by at least 60 K. The middle heavy curve is a copy of the heavy curve in Fig. 1.

The contrast between the curves suggests that if l had been increased rather than decreased, the multiple equilibria might have disappeared altogether. This proves to be the case; the left-hand heavy curve in Fig. 2 has been constructed from runs where $lv/\lambda = 0.06$.

The variations of the equilibrium curve are in qualitative agreement with what one might expect if a cloud–albedo process is operating. The low value of l corresponds to clouds which experience some difficulty in precipitating their water, and consequently tend to persist. The high value of l, which does not produce multiple equilibria, corresponds to clouds which are rapidly attenuated by precipitation, so that the cloud–albedo feedback process is also attenuated. At some value of l the model evidently undergoes a transition between regimes, one where multiple equilibria occur and the other where T is merely highly sensitive to T^*.

Are the multiple equilibria realistic? They do not agree with what we have seen in our own atmosphere. The cold equilibria are so cold that the oceans would be frozen over, while the warm equilibria are so warm that the implicit assumption that the mixing ratios are small would break down. However, the real atmosphere always possesses a circulation, transporting excess heat from warm to cold regions, and we do not know what would happen if the heating could be made horizontally uniform, although our guess is that we would be in the high-l regime.

For good measure we have added two more curves to Fig. 2, corresponding to halved and doubled values of k. Qualitatively, lowering k is like raising l, but the effect is much smaller. We have also made computations with $a = r^2$, obtaining a curve much like the right-hand heavy curve. Letting $a = r^2/2$ removes the multiple equilibria and produces a curve like the left-hand heavy curve, but we prefer a formulation where $a \to 1$ as $w \to \infty$. Including a surface albedo in the model might further complicate the feedback process, as indicated, for example, by the analysis of Stephens and Webster (1981).

In our remaining computations the solar heating varies with latitude; we have let $T^* = T_0^*\Phi_0 + T_3^*\Phi_3$, with $T_0^* = 273.0$ K and $T_3^* = 5.0$ K. According to (28) the values of T^* at the southern and northern grid points are therefore about 267 and 279 K, respectively. Reference to Table 1 shows that the equilibrium temperatures are about 248 and 313 K. Although we would expect the circulation to prevent such a large contrast in T from developing, we should not be surprised if T_3 [defined in Eqs. (27) and (28)] exceeds T_3^*.

For initial conditions in our first run we have superposed a fairly small wave disturbance $T_1 = W_1 = S_1 = 1.0$ K on the zonally symmetric (but not steady) circulation $\psi = 0$, $T = W = S = T^*$. We have used the four-cycle scheme (Lorenz, 1971) with $\delta t = 1.5$ h and $\Delta t = 6$ h. Table 2 shows the development of the temperature field during the 500 days of the run.

During the first 20 days the mean temperature T_0 drops, at first rapidly, apparently in response to an unbalance between T_0 and S_0, and then rather slowly. As anticipated, the cross-latitude contrast T_3 proceeds to grow. The superposed wave damps considerably, and, as indicated by the succession of plus and minus signs in T_1 and T_2, and T_4 and T_5, progresses eastward slightly more than a full wavelength.

This behavior continues until the third month, when the wave is rejuvenated, soon surpassing its original amplitude. Presumably the growth takes place because T_3 has increased to the point where the zonal flow is baroclinically unstable. As the wave continues to extract energy from the zonal flow during the fourth month, T_3 decreases, thereafter oscillating about a baroclinically neutral value. Meanwhile, T_4, T_5 and T_6 begin to assume appreciable values. It is noteworthy that with the chosen initial conditions these variables would have continued to vanish in a model whose only nonlinear process is advection by the geostrophic wind.

During the second half-year T_6 becomes decidedly negative, indicating, since T_3 is strongly positive, that the cross-latitude temperature gradient is largest in high latitudes. Evidently a stronger temperature gradient is required for baroclinic instability under these conditions, since T_3 now oscillates about a larger value. There appears to be a 120-day period in the oscillations; however, examination of daily values from days 480 to 500 has revealed that the period is actually about

TABLE 2. Values of temperature coefficients $T_0, \ldots, T_6$ (K), at selected times t (days), in the first numerical run with the low-order model, with $T^* = 273.0 + 5.0\Phi_3$.

t	T_0	T_1	T_2	T_3	T_4	T_5	T_6
0	273.00	1.00	0.00	5.00	0.00	0.00	0.00
4	272.05	0.22	0.78	5.46	0.02	0.00	0.02
8	271.83	−0.49	0.30	5.72	−0.01	0.03	0.02
12	271.73	−0.30	−0.28	5.96	−0.03	−0.02	0.03
16	271.64	0.13	−0.22	6.18	0.02	−0.02	0.04
20	271.55	0.14	0.08	6.40	0.00	0.02	0.06
40	271.12	−0.02	0.01	8.46	0.00	0.00	0.16
60	270.74	0.01	0.02	8.48	0.00	0.00	0.28
80	270.43	−0.11	0.15	9.48	−0.01	0.01	0.39
100	271.58	2.43	−1.61	8.48	−0.40	0.46	0.33
120	272.54	1.35	−1.62	8.53	−0.23	0.13	−0.84
180	272.19	−0.12	0.02	10.06	−0.10	0.33	−1.87
240	272.35	−0.72	−0.22	10.67	0.39	0.04	−2.12
300	272.74	−0.19	−0.19	10.35	−0.61	−0.05	−2.17
360	272.98	−0.68	−0.10	10.54	0.31	0.08	−2.02
420	273.32	−0.16	−0.15	10.31	−0.64	−0.01	−2.21
480	273.52	−0.62	0.10	10.59	0.29	−0.06	−2.03

TABLE 3. Values of temperature coefficients $T_0, \ldots, T_6$ (K), at selected times t (days), in the second numerical run with the low-order model, with $T^* = 273.0 + 5.0\Phi_3$.

t	T_0	T_1	T_2	T_3	T_4	T_5	T_6
0	283.68	−0.19	−0.17	10.33	−0.63	0.13	−2.19
30	284.77	0.12	−0.06	9.28	−0.47	−0.37	−2.39
60	284.79	−0.03	0.25	8.76	0.38	−0.34	−2.25
90	284.72	0.03	0.26	8.74	0.18	−0.44	−2.15
120	284.60	0.07	0.20	9.04	0.07	−0.44	−2.09
150	284.44	−0.10	0.07	9.56	0.40	0.05	−2.04
180	284.19	0.09	0.03	10.35	−0.06	−0.36	−1.96
210	283.77	−0.03	0.01	11.65	0.11	0.16	−1.83
240	283.96	0.28	−1.26	11.11	−0.59	−0.89	−2.70
270	283.71	−0.40	−0.02	8.51	0.50	−0.14	−2.49
300	283.69	0.11	0.24	8.15	−0.18	−0.43	−2.22
330	283.60	−0.10	−0.04	8.59	0.00	0.39	−2.08
360	283.32	−0.06	−0.08	9.57	−0.08	0.30	−1.92
390	282.64	0.01	0.00	11.11	0.00	0.13	−1.59
420	282.82	−0.49	0.56	10.40	−0.90	0.26	−2.78
450	283.00	0.43	0.00	8.73	−0.51	−0.09	−2.40
480	282.97	0.27	−0.14	8.57	−0.46	0.07	−2.19

13 days; nine cycles rather than one occur between days 360 and 480. Superposed on this oscillation there is an upward trend of about 1.5 K per year in T_0, suggesting that transient effects have not yet disappeared.

Instead of continuing the run to equilibrium, which would require several simulated years, we have performed a second 500-day run, whose initial conditions are the final conditions of the first run with 10.0 K added to T_0, W_0 and S_0. Table 3 shows what happens. After an initial adjustment, T_0 drops while the waves decay. In response, T_3 increases, until, after day 200, baroclinic instability sets in, whereupon the wave becomes strong again and T_3 decreases. This set of events is repeated 180 days later. Examination of daily values from days 480 to 500 shows no appreciable short-period oscillation. A downward trend in T_0 is comparable in magnitude to the upward trend in the first run.

For initial conditions in our final run we have used the final conditions of the second run with 4.0 K subtracted from T_0, W_0 and S_0. During the 500 days T_0 fluctuates but shows no appreciable trend. Statistically-stationary behavior appears to have been reached.

In Table 4 we present values of all the prognostic variables for the final state of each run. These states have certain features in common, which also prevail throughout most of each run. First, $W_0 < T_0$; as a consequence the globally averaged relative humidity and the global albedo fall short of the values 0.80 and 0.41 which would prevail with $W = T$; for the three final states the global albedos are 0.37, 0.31 and 0.34.

As indicated by the plus and minus signs in the coefficients of T_1 and T_2, the waves in the T-field are generally displaced westward from those in the ψ-field (the coefficients of T_4 and T_5 are less consistent), while the W-field waves are well to the west of the T-field waves. Thus the most humid air is flowing with a component from the south. A striking feature which we had not anticipated is the consistently larger amplitude of the W-field waves than the T-field waves. It is not surprising that the S-field waves are weak; they are forced by the atmospheric waves, which move too fast to allow much build-up in the ocean.

Figure 3 translates the final tabulated state into synoptic charts, covering somewhat more than one wavelength. There are well formed cyclones and anticyclones at 1000 mb; the 15 m spacing for the height contours, derived geostrophically from ψ, is equivalent to about a 2 mb spacing for sea-level isobars. The isotherms

TABLE 4. Values of coefficients ψ_i, T_i, W_i and S_i (K), for $i = 1, \ldots, 6$, at final time in each of three runs with the low-order model, with $T^* = 273.0 + 5.0\Phi_3$ (for streamfunction ψ, 1 K = 0.01 dimensionless units = 3.10×10^6 m^2 s^{-1}, geostrophically equivalent to 29.3 m in 1000 mb height).

	i						
Run	0	1	2	3	4	5	6
1:							
ψ_i	0.00	0.36	−0.22	0.12	−0.19	0.09	−0.42
T_i	273.68	−0.19	−0.17	10.33	−0.63	0.13	−2.19
W_i	272.92	−1.92	−0.46	9.29	1.72	1.10	−1.22
S_i	275.44	−0.04	0.03	9.40	−0.04	0.18	−1.97
2:							
ψ_i	0.00	0.00	0.35	−0.12	0.00	−0.12	−0.10
T_i	282.88	0.07	0.20	8.88	−0.01	0.42	−2.09
W_i	281.00	1.36	−1.02	7.73	−1.09	0.63	−1.40
S_i	283.17	0.02	0.04	7.68	−0.10	−0.04	−1.76
3:							
ψ_i	0.00	0.08	−0.53	−0.05	−0.08	0.11	−0.13
T_i	278.56	−0.44	−0.50	10.74	0.11	0.39	−2.11
W_i	277.12	−1.43	1.68	9.49	0.97	−0.54	−1.69
S_i	279.50	−0.13	0.02	9.93	0.09	0.04	−1.94

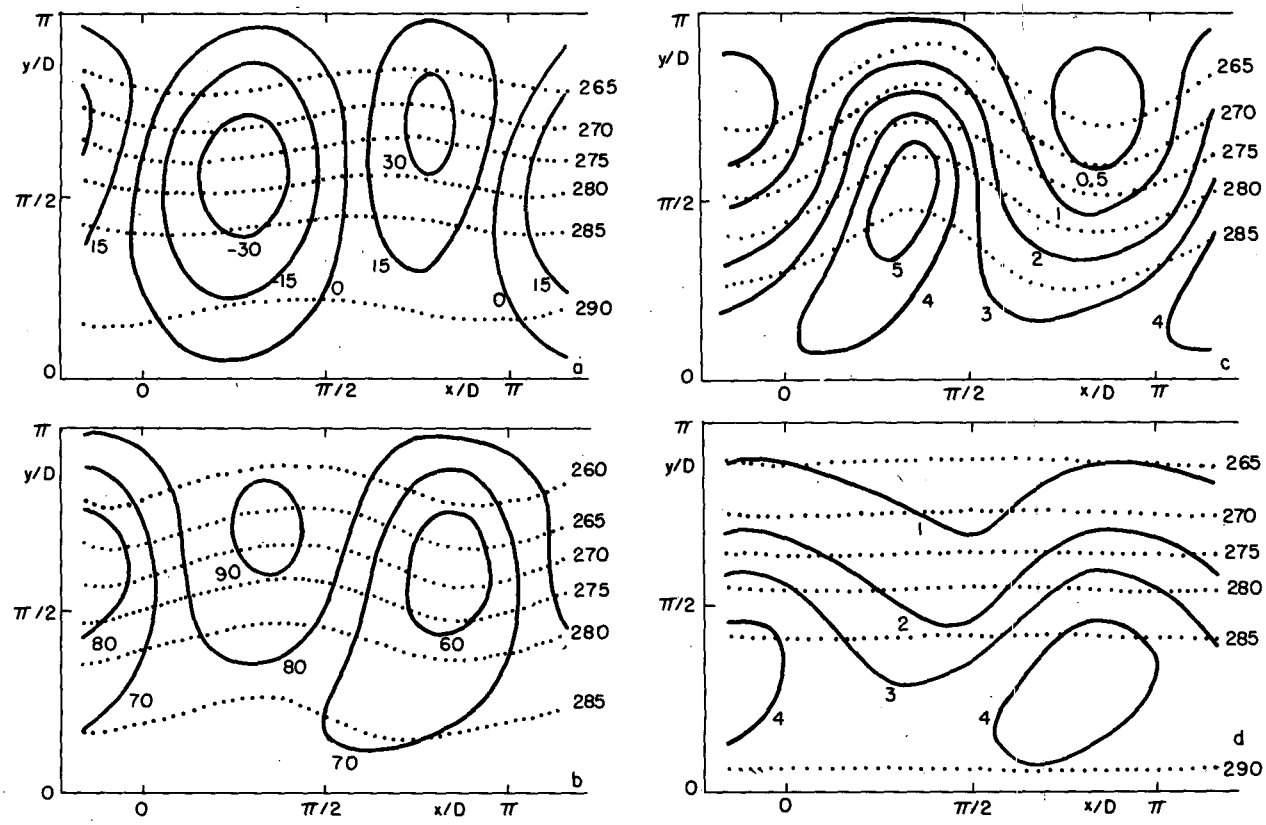

FIG. 3. Fields at end of third model run. (a) 1000 mb height (solid curves, interior labels in m), and 1000 mb temperature (dotted curves, labels at right in K). (b) 1000 mb relative humidity (solid curves, interior labels in %), and 1000 mb dew point (dotted curves, labels at right in K). (c) Precipitation (solid curves, interior labels in mm day^{-1}), and 1000 mb total dew point (dotted curves, labels at right in K). (d) Evaporation (solid curves, interior labels in mm day^{-1}), and ocean surface temperature (dotted curves, labels at right in K).

are fairly zonal, but the air is a few degrees warmer to the west of the anticyclones and cooler to the west of the cyclones.

The waves in the dew-point field and especially the total-dew-point field are more pronounced, while waves in the sea-surface temperature field are virtually absent. The relative-humidity field possesses a moist center north-northeast of the 1000 mb cyclone and a dry center south-southeast of the anticyclone, while the maximum precipitation is somewhat south of the moist center and the minimum is somewhat north of the dry center. The evaporation exhibits less variability than the precipitation.

The longitudinal variations in Fig. 3 are rather weak by real atmospheric standards. We have yet to determine whether this is due principally to an excessively high static stability, a weak cross-latitude heating contrast, or some other cause. At times the systems are stronger; on day 240 in the second run, for example, the sea-level pressure varies from 984 to 1014 mb, the relative humidity from 31 to 96%, and the precipitation rate from 0.1 to 12.5 mm day^{-1}. Qualitatively we find the behavior reasonable, and we conclude tentatively that the model is suitable for production runs.

7. Concluding remarks

Our model has undergone considerable evolution during its development, and the evolution need not cease at this point. Some changes ought to be made in any experiments where closer quantitative resemblance to the earth's atmosphere is desired. We might tune the model by changing the values of some of the constants, or we might add such physical features as reflection of shortwave radiation by the ocean or absorption of longwave radiation by carbon dioxide. Such changes would make the model conceptually somewhat more complicated, but they would not noticeably affect the amount of computation per time step.

More important are changes which would improve the model for general purposes. We feel that the principal shortcoming at present is the assumption of a uniform prechosen lapse rate of temperature. Amplifying waves should limit their own ultimate growth by making the zonal flow on which they are superposed less unstable baroclinically, and one way in which they may do so is by transporting heat upwards, thereby stabilizing the lapse rate.

In our vacillation model (Lorenz, 1963), we allowed

the lapse rate to vary with time but not spatially. With a prechosen lapse rate we could not have simulated the stable behavior which is observed in the associated laboratory experiments (Fultz *et al.*, 1959) when the heating is strong. We could modify the present model by making λ a function λ_0 of time alone, deriving a governing equation for λ_0 from (6) or (7) or some combination of (6) and (7). Vertical transport of heat would then alter λ_0. Unfortunately, we would also have to make some assumption regarding the vertical radiative flux within the atmosphere—an assumption which we have been trying to avoid. The model would become somewhat more cumbersome, but we see no insuperable difficulties. Allowing λ to vary horizontally would greatly complicate the model.

Finally, we may question whether we have really accomplished our goals of simplicity in concept, formulation and execution. Certainly the model is far more complicated than the dry vacillation model, and the execution is an order of magnitude slower. It could presumably be speeded up by replacing some of the more complicated functions by tables, and by using interpolation, but we see no way to simplify the formulation appreciably without weakening the model. In models of local circulations (e.g., Shirer and Dutton, 1979) where the total range of temperature is not too great, assumptions such as a constant value of the moist adiabatic lapse rate, perhaps half of the dry adiabatic, have been profitably used. In a model extending from tropical to polar latitudes, such assumptions could be counter-productive.

Acknowledgment. This research has been supported by the Air Force Geophysics Laboratory, Air Force Systems Command, under Contracts F19628-81-K-0001 and F19628-83-K-0012.

REFERENCES

Fultz, D., R. R. Long, G. V. Owens, W. Bohan, R. Kaylor and J. Weil, 1959: *Studies of Thermal Convection in a Rotating Cylinder with some Implications for Large-Scale Atmospheric Motions. Meteor. Monogr.*, No. 21, Amer. Meteor. Soc., 104 pp.

Held, I. M., and M. J. Suarez, 1978: A two-level primitive-equation atmospheric model designed for climatic sensitivity experiments. *J. Atmos. Sci.*, **35**, 206–229.

Lorenz, E. N., 1963: The mechanics of vacillation. *J. Atmos. Sci.*, **20**, 448–464.

——, 1971: An *N*-cycle time-differencing scheme for stepwise numerical integration. *Mon. Wea. Rev.*, **99**, 644–648.

——, 1982: Low-order models of atmospheric circulations. *J. Meteor. Soc. Japan*, **60**, 255–267.

Platzman, G. W., 1960: The spectral form of the vorticity equation. *J. Meteor.*, **17**, 635–644.

Shirer, H. N., and J. A. Dutton, 1979: The branching hierarchy of multiple solutions in a model of moist convection. *J. Atmos. Sci.*, **36**, 1705–1721.

Simpson, G. C., 1928: Further studies in terrestrial radiation. *Mem. Roy. Meteor. Soc.*, Vol. 3, No. 21, 26 pp.

Stephens, G. L., and P. J. Webster, 1981: Clouds and climate: Sensitivity of simple systems. *J. Atmos. Sci.*, **38**, 235–247.